

# Is the dry-band characteristic a function of pollution and insulator design?

M. Albano<sup>1</sup>, A.Haddad<sup>1</sup>, N. Bungay<sup>1</sup>

<sup>1</sup> Cardiff University  
The Parade, Cardiff, UK  
[albanom@cardiff.ac.uk](mailto:albanom@cardiff.ac.uk)

**Abstract:** This research work aims to assess whether dry-band formation and location are function of pollution level with the application of new insulator surface design. Artificial pollution tests have been performed on a 4-shed 11kV insulators with conventional and textured surface designs in clean-fog chamber and a voltage ramp shape source. The statistical location and extension of the dry-bands during these comparative tests have been analysed and it may offer good suggestions to establish design guidelines in dry-band control.

## I. INTRODUCTION

Pollution is a significant problem for high voltage insulators that can impact significantly the availability of a high voltage transmission line. The adoption of silicone rubber insulators offers improved performance under severe polluted environment. However the superior performances of this material are reduced when dry-bands appear and discharge activity is established on the insulator area, determining a localised reduction of the hydrophobic properties of the silicone rubber. If this activity persists, the partial arcs can initiate localized erosion, weakening the insulator surface, as shown in several researches [1-5].

The importance of this topic is shown by numerous recent works on dry-bands [6-9]; where the influence of dry band on flashover characteristics under various environmental and pollution conditions is investigated on rectangular silicone rubber samples.

In this research work artificial pollution tests have been performed on a 4-shed 11kV insulators and various designs in clean-fog chamber using a wide range of pollution levels and the statistical location of the dry-bands have been analysed. Further characteristics, as width and temperature distribution, have been investigated; infrared recording during the tests have been processed using a developed Matlab procedure in order to identify the width of each dry-band and to monitor its variation during the entire test. The series of clean-fog tests have been performed adopting conventional and textured designs. In addition, equivalent salt deposit density after the application of artificial pollution layer have been determined on all selected insulator designs to investigate its contribution on the dry-band characteristics and location. These comparative tests may offer good suggestions to establish design guidelines in dry-band control.<sup>1</sup>

## II. EXPERIMENTAL SET UP

The laboratory test method selected for this research work uses a clean fog chamber and a voltage ramp shape source applied on artificial polluted insulators. The high voltage source is Hipotronics 150kVA transformer able to provide programmed voltage variation up to 75kV. In this series of tests the voltage is applied with a constant increase of 4 kV per minute to achieve the ramp shape; this permits to assess the insulator performance under increasing stress in limited period of time. This method has been developed by Cardiff University research team and described in details in [10]. Previous works evaluated the impact of fog rate and pollution level applied as ESDD and NSDD on the insulator surface. In addition, the voltage ramp test in clean fog has been extensively adopted to assess the impact on withstand of textured design versus plain surface. These series of tests showed clear indication of improved flashover withstand performance of textured insulators in comparison with conventional surfaces [11]. Table I shows the geometrical dimensions of the insulators selected for this investigation. It is important to note the increased creepage length offered by texturing the surface of the insulator (TT). Further increased creepage length is offered in TTS design, applying a logarithmic spiral double-ridge pattern. The plain surface insulator, conventional design, is labelled as CONV.

TABLE I  
INSULATOR DESIGNS

Design	Creepage length (mm)	Dimple size radius (mm)	Under shed profile (mm)
CONV	375	0	0
TT4	471	4	4
TTS4	503	4	4
TT6	471	6	6
TTS6	503	6	6

During the tests visual images were taken with a High Definition visual camera in order to identify and visualize indications of the discharge phenomena, nearby the dry-band, that is not clearly visible in the optical range. Simultaneously IR pictures were recorded using the FLIR A325 camera every

second. The camera has the capability to monitor the temperature at a frequency rate up to 60Hz and with a precision of 0.5 °C. These capabilities are clearly not sufficient to record the instantaneous maximum temperature of the discharge but the IR records can show with good precision the maximum temperature of the insulator surface; the time stamp associated with each IR-frame recorded help to synchronize the temperature with other data recorded during the test, as electrical parameters and the visual records, with a precision of 1 ms.

### III. EXPERIMENTAL RESULTS AND DRY-BAND DETECTION PROCEDURE

A series of laboratory tests were performed using the selected insulator designs with the application of severe, high and moderate pollution level, 1.15, 0.64 and 0.42 mg/cm<sup>2</sup> respectively.

In the initial tests, some discharge activities were identified using long exposure digital camera, as shown in Figure 1. These small discharges were not visible in the digital camera recording but only in the photo; the associated dry-band were localized only with the help of the IR camera. The visual photos were post processed in order to enhance the spark visibility. Two different type of discharges are shown, a corona streamer, purple-blue in the photo, in the same area of the dry-band, and streamer discharges, red-orange colour, crossing wider area than the dry band.

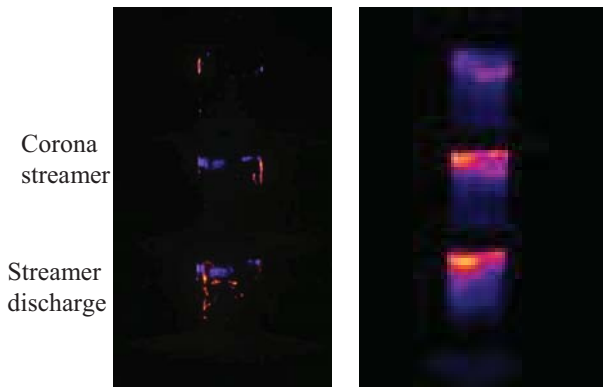


**Figure 1.** Visual (left) and IR (right) records of sample TT4 test, ESDD 0.64 mg/cm<sup>2</sup>, fog spray rate 3 l/h.

The IR image recorded simultaneously showed where the presence of fully formed dry-bands as area of increased temperature, as shown in Figure 1 (right). It is worth to note that the upper trunk does not show significant streamer activity, however the IR photo shows the presence of dry band in each trunk, with less intensity on the top one. Figure 2 shows the temperature difference between insulator surface and fog. If simply a threshold of 5.5 °C is selected as identification method, no dry-bands would be detected in this temperature profile.

In addition, the manual processing to identify the dry band is very time consuming, and the need to process a significant

number of frames and series of tests suggested the need of developing an automatic procedure.

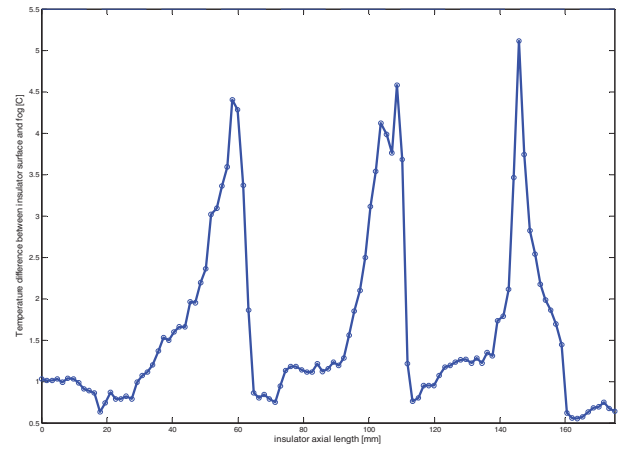


**Figure 2.** Temperature difference between insulator surface and fog.

Two main features can be calculated from the IR records, the maximum temperature on the insulator surface during the tests and the average temperature on selected areas.

The analysis of the thermal data cannot be limited to the variation of the maximum temperature during the test, since this can help to identify only the spark / dry-bands events in time but not their location, extension or number.

For this reason the authors developed an automatic procedure to analyze the temperature variation on different areas of the insulator. Initial tests showed that the trunks are statistically more subjected to dry-band event and corona discharge than sheds, therefore the analysis was focused mainly on these areas.

#### A. Automatic boundaries recognition

An important part of the analysis is the correct identification of the insulator position on the IR record and its outline. Since the insulator and the fog are at close temperature values at the start of the test, the automatic identification is not a trivial task. In addition, possible reflections on the object can cause significant error in the outline identifications.

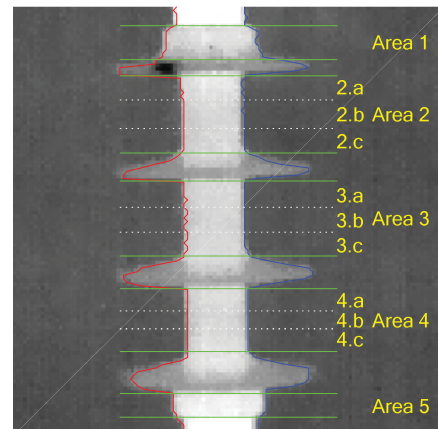


**Figure 3.** Automatic boundaries recognition and areas selection.

A semi-automatic procedure followed by user interaction to confirm and finalize the areas has been selected. The boundary detection system is based on Matlab procedure developed in-house analyzing the small temperature variation between the fog and the insulator. Each trunk area has been subdivided in three zones (a, b, c), as shown in Figure 3. The area a is characterized by the presence of the shed, the area b is the central area, more exposed to the wetting action by the fog and the remaining one, c, is near the top shed zone.

**B. Average temperatures**

The procedure identifies in the IR temperature data the values related to each area and calculate the average temperature for each frame, as shown in Figure 4. The average temperature of the three trunk areas and the two end fitting areas during the whole tests are aggregated in two subplots to facilitate the comparison. It can be observed that after an initial cooling period, there is a steady increase in dry-band width as the voltage/current increases. The polluted insulator initially stored at laboratory temperature is then placed during the test in the fog chamber where the fog cools the insulator surface, until the discharge activity heats up. From the plot the different temperature trend is clearly visible in area 4 and in area 5, suggesting the present of dry-band and between 4 and 5 minutes there is a noticeable rapid increase in dry-band sizes.

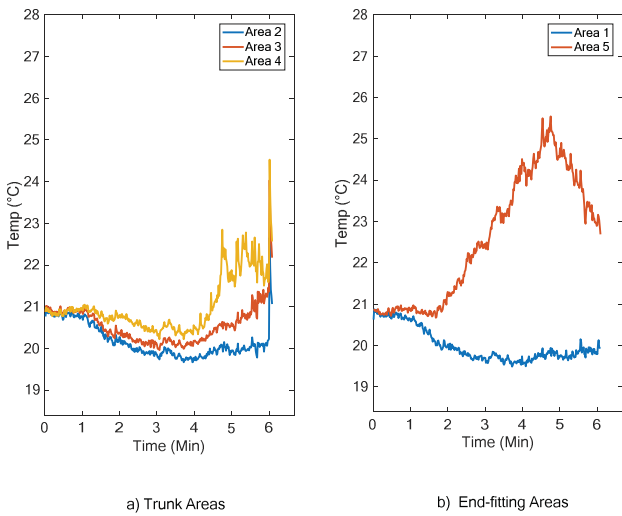


**Figure 4.** Average temperature of trunk areas and end fitting areas during the whole test.

Figure 5 shows the average temperature of selected sub-areas of each trunk during the whole test. The shape of the graph looks very similar to the previous figure but the subdivision into sub-areas can help to identify different wetting rate and different pollution accumulation on live use. The figure shows clearly that the Area 4 sub area a) is presenting a localised heating as a dry-band. This approach is very useful for comparative tests of different designs.

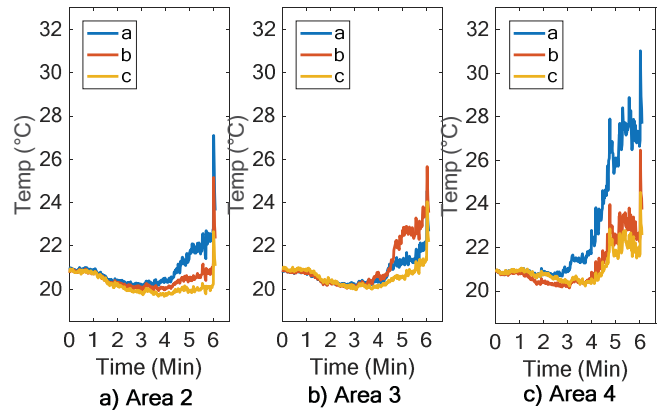


**Figure 5.** Average temperature of selected sub-areas of each trunk during the whole test

Another clear indication from the average temperature of subareas is that the sub-area c presents always the lower average temperature in each trunk. This suggests that the wetting is more facilitated than in the other two sub areas, meanwhile in the area closer to the shed the wetting is slightly reduced creating better condition for dry-band formation.

**C. Dry-band analysis**

Another important information is the localisation and development of any dry-band during the test. The detection of dry band using a selected threshold is not always correct, as shown in the temperature profile described in Figure 2. In addition using a variable level function only on the first IR frame is still not always applicable since the fog cooling effect. The algorithm detection is based on exceeding the average value taking into account of the cooling effect in the initial period. Each dry band width is evaluated counting the number of IR pixel exceeding this threshold and converting the number of pixel in mm, from the known vertical height of the insulator, 175 mm. The total dry-band extension along the vertical axis is an interesting parameter to calculate, as shown in Figure 6.

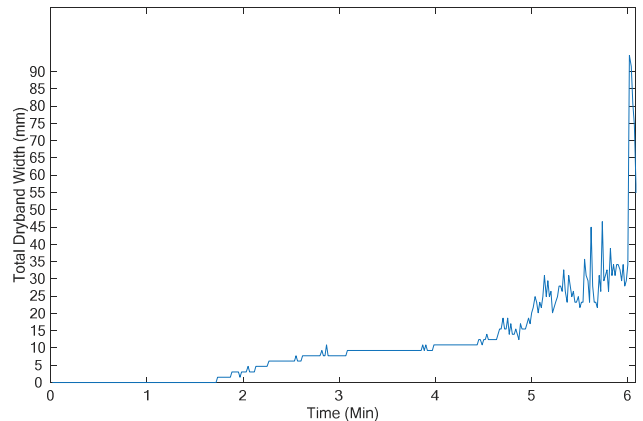


**Figure 6.** Total dry-band length

#### IV. CONCLUSIONS

The presented research work showed that dry-band formation and location are function of the application surface design given a selected pollution level (ESDD).

Pollution level is one of the important parameter in the insulator selection, however another important aspect is the life expectancy. Life expectancy is one of the key parameter that utilities have to evaluate before applying new design. Since, one of the major cause of degradation on polymeric insulators is caused by discharges on the surface, this IR video analysis and characterization of dry band may provide useful indication of the selection of the most appropriate surface design to maximize the insulator life extension.

#### REFERENCES

- [1] R. S. Gorur, E. A. Cherney, R. Hackam, T. Orbeck, "The Electrical Performance of Polymeric Insulating Materials Under Accelerated Aging in a Fog Chamber", *IEEE Trans. on Power Delivery*, vol. 3, no. 3, pp. 1157-1163, 1988.
- [2] V.M. Moreno, R.S. Gorur, "Effect of long-term corona on non-ceramic outdoor insulator housing materials", *Dielectrics and Electrical Insulation IEEE Transactions on*, vol. 8, no. 1, pp. 117-128, 2001.
- [3] P. Blackmore and D. Birtwhistle, "Surface discharges on polymeric insulator shed surfaces", *IEEE Transactions on Dielectrics and Electrical Insulation*, vol. 4, no. 2, pp. 210-217, Apr 1997. doi: 10.1109/94.595248
- [4] V.M. Moreno, R.S. Gorur, "Impact of corona on the long-term performance of nonceramic insulators", *Dielectrics and Electrical Insulation IEEE Transactions on*, vol. 10, no. 1, pp. 80-95, 2003.
- [5] Delun Meng, Boveri-Yibo Zhang, Jiansheng Chen, Seung-Chul Lee, Jong-Yun Lim, "Tracking and erosion properties evaluation of polymeric insulating materials", *High Voltage Engineering and Application (ICHVE) 2016 IEEE International Conference on*, pp. 1-4, 2016.
- [6] N. Dhahbi-Megrache, M. E. A. Slama and A. Beroual, "Influence of dry bands on polluted insulator performance," *2017 International Conference on Engineering & MIS (ICEMIS)*, Monastir, 2017, pp. 1-4. doi: 10.1109/ICEMIS.2017.
- [7] Arshad, A. Nekahi, S.G. McMeekin and M. Farzaneh, "Influence of Dry Band Width and Location on Flashover Characteristics of Silicone Rubber Insulators", *2016 Electrical Insulation Conference (EIC)*, Montréal, Qc, Canada, 19 - 22 June 2016.
- [8] Arshad, Nekahi, A., McMeekin, S.G. et al., "Measurement of surface resistance of silicone rubber sheets under polluted and dry band conditions", *Electr Eng* (2017)
- [9] Arshad, M. Mughal, A. Nekahi, M. Khan, and F. Umer, "Influence of Single and Multiple Dry Bands on Critical Flashover Voltage of Silicone Rubber Outdoor Insulators: Simulation and Experimental Study," *Energies*, vol. 11, no. 6, p. 1335, May 2018.
- [10] P. Charalampidis, M. Albano, H. Griffiths, A.M. Haddad, R.T. Waters, "Silicone Rubber Insulators for Polluted Environments Part 1: Enhanced Artificial Pollution Tests", *IEEE Transactions on Dielectrics and Electrical Insulation*, Vol. 21, Issue 2, pp. 740-748, April 2014, DOI: 10.1109/TDEI.2013.004015.
- [11] M. Albano, P. Charalampidis, H. Griffiths, A.M. Haddad, R.T. Waters, "Silicone Rubber Insulators for Polluted Environments Part 2: Textured Insulators", *IEEE Transactions on Dielectrics and Electrical Insulation*, Vol. 21, Issue 2, pp. 749-757, April 2014, DOI: 10.1109/TDEI.2013.004016.

In order to estimate the effect of the design on the dry-band extension, the total dry-band extension for selected designs for a given ESDD and fog spray rate can be plotted as shown in Figure 7. It is clear that the CONV design presents dry-band formation much earlier than textured insulators, just after 1 minutes the CONV samples start to show dry-bands and continue to extend with increasing voltage. The trend is significantly delayed on TT samples, where the total-dry-band length is start to be significant after 4 min. The minutes preceding the flashover, show an interesting trend, the dry-bands on the TT6 design have increased extension whereas TT4 and TTS4 show the most delayed increased and lower maximum length before flashover. If the analysis would have been limited only to flashover breakdown voltage, the test results would have not shown such strong difference as in this figure.

In order to understand with more precision, the growth of each dry-band has been analysed in the Matlab procedure and plotted as in Figure 8. This graph is very useful, since each dry-band width is plotted as function of time and as its dry-band temperature range. This graph permits to compare the dry-band temperature distribution of specific tests very easily.

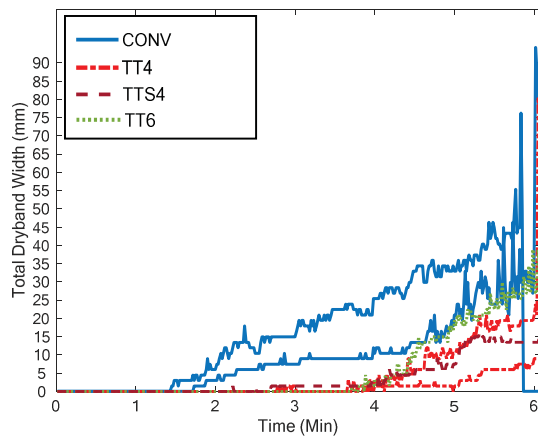


**Figure 7.** Total dry-band extension for different designs, ESDD  $0.64 \text{ mg/cm}^2$ , fog spray rate 3 l/h.

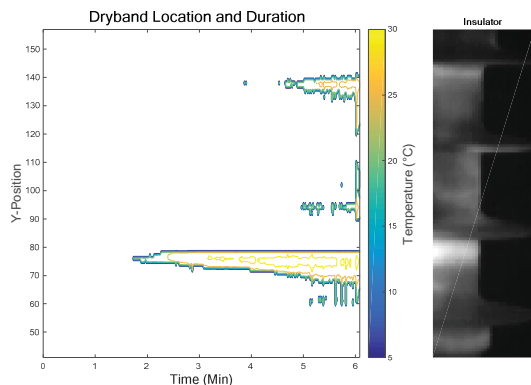


**Figure 8.** Example of individual dry-band extension function of time and dry-band temperature range.